Brain Structure and Function (2020) 225:1089–1102
https://doi.org/10.1007/s00429-020-02061-2

ORIGINAL ARTICLE

ALE meta-analysis, its role in node identification and the effects on estimates of local network organization

Dimitri Falco[1] · Asadur Chowdury[2] · David R. Rosenberg[2] · Steven L. Bressler[1,3] · Vaibhav A. Diwadkar[2]

Received: 18 September 2019 / Accepted: 20 March 2020 / Published online: 3 April 2020

Abstract

Functional connectivity analyses for task-based fMRI data are generally preceded by methods for identification of network nodes. As there is no general *canonical* approach to identifying network nodes, different identification techniques may exert different effects on inferences drawn regarding functional network properties. Here, we compared the impact of two different node identification techniques on estimates of local node importance (based on Degree Centrality, DC) in two working memory domains: verbal and visual. The two techniques compared were the commonly used Activation Likelihood Estimate (ALE) technique (with node locations based on data aggregation), against a hybrid technique, Experimentally Derived Estimation (EDE). In the latter, ALE was first used to isolate regions of interest; then *participant-specific* nodes were identified based on individual-participant local maxima. Time series were extracted at each node for each dataset and subsequently used in functional connectivity analysis to: (1) assess the impact of choice of technique on estimates of DC, and (2) assess the difference between the techniques in the ranking of nodes (based on DC) in the networks they produced. In both domains, we found a significant Technique by Node interaction, signifying that the two techniques yielded networks with different DC estimates. Moreover, for the majority of participants, node rankings were uncorrelated between the two techniques (85% for the verbal working memory task and 92% for the visual working memory task). The latter effect is direct evidence that the identification techniques produced different rankings *at the level of individual participants*. These results indicate that node choice in task-based fMRI data exerts downstream effects that will impact interpretation and reverse inference regarding brain function.

Keywords Node identification · Activation likelihood estimates · Individual differences · Degree centrality

Introduction

Meta-analysis is a central tool for summarizing task-based fMRI data (Genon et al. 2018). Methods such as Activation Likelihood Estimates (ALE) now reliably identify activation loci (nodes) across multiple independent studies under the same task paradigm, i.e., hundreds of studies and thousands of participants (Eickhoff et al. 2012). These co-activated nodes are effectively treated as a reliable task-activated network of regions, that can then be deployed for analyses such as meta-analytic connectivity modeling (Langner et al. 2014; Robinson et al. 2010). Thus, task-constrained co-activated nodes can be used in the service of assessing functional connectivity (primarily in resting-state fMRI data, Mancuso et al. 2019). ALE can be a highly valuable tool for data summarization in one domain of big data (such as working memory, e.g., Owen et al. 2005) to then constrain investigations of connectivity in a complimentary domain of big data

Electronic supplementary material The online version of this article (https://doi.org/10.1007/s00429-020-02061-2) contains supplementary material, which is available to authorized users.

✉ Vaibhav A. Diwadkar
vdiwadka@med.wayne.edu

[1] Center for Complex Systems and Brain Sciences, Florida Atlantic University, Boca Raton, FL, USA

[2] Brain Imaging Research Division, Department of Psychiatry and Behavioral Neuroscience, Wayne State University School of Medicine, Suite 5A, Tolan Park Medical Building, 3901 Chrysler Service Drive, Detroit, MI 48201, USA

[3] Department of Psychology, Florida Atlantic University, Boca Raton, FL, USA

(e.g., resting-state fMRI data). However, the value of ALE (over and above complementary methods) in deriving the most appropriate estimates of *network connectivity* within any specific task-active data set is unclear. That is, while the nodes may reliably represent *activation* loci for a specific task domain, are they the appropriate representations of an *individual's* network connectivity?

Node identification is an important step within any specifically acquired task-based data set, because task-induced modulation of network *connectivity* is not completely predicted by co-activated nodes (Morris et al. 2018) and may be subject to significant individual variation. Indeed, recent studies (Falco et al. 2019), have investigated the effects of ALE-derived networks (against individual-specific networks) on estimates of functional connectivity, and like other studies (Mueller et al. 2013; Finn et al. 2015) have found that estimates of functional connectivity are dominated by individual differences. Thus, because discovery of network characteristics is "downstream" from the identification of network nodes, the effects of choices made in identifying network nodes must be characterized.

Graph theoretic approaches (Rubinov and Sporns 2010), can help in summarizing these effects on nodes and/or edges (i.e., estimates of connectivity). One choice involved in identifying networks is to determine a reasonable number of candidate nodes. For example, *each* voxel in the brain can be considered a putative network node, but the resulting network size (~ 130,000 nodes) would make it intractable to measure *all* edges. Brain parcellation schemes (Thirion et al. 2014) reduce the network space by averaging fMRI signals across voxels within a parcel. However, principles of relative specialization of function (Friston 2003) mean that large numbers of parcels in task-based fMRI data are *unrepresentative* of task-related activity. Furthermore, the identification of network nodes should take into consideration the relationship between the existence of shared functional information in adjacent voxels, where neighboring voxels tend to have highly correlated functional measures. These considerations, among others, motivate the use of data summarization techniques (such as ALE).

Approaches for identifying networks

A recent study (Falco et al. 2019) compared ALE against a "hybrid" experimentally derived estimation (EDE) technique in the working memory domain. In the hybrid technique, ALE nodes were mapped to anatomical regions of interest, from which participant-specific activation peaks were then utilized as nodes for subsequent assessment of functional connectivity. This approach retained the statistical power (through data aggregation) of ALE to narrow loci to regions of interest, while also ensuring that nodes were selected from *unique individual* activation maxima. The techniques led to two distinct networks from the fMRI BOLD data of each participant: an ALE-derived network (by nature "fixed" across participants), and an EDE-derived network that could be unique for each participant (based on individual-participant activation maxima). The techniques used to define the nodes exerted clear effects on the inferences regarding undirected functional connectivity (based on bivariate correlation models; Silverstein et al. 2016), that is *edges* in the network. What was not quantified was the effect of these choices on the relative organization of the *nodes* themselves.

Degree centrality

As implicitly noted, the brain's widespread structural and functional connectivity (Park and Friston 2013) makes it a prototypical example of a graph with nodes (brain regions) and edges (structural and/or functional connections between regions). Brain regions have distinct 'functional fingerprints' that emerge in response to patterns of network connectivity (Bressler 2002; Passingham 2002), and these patterns can be effectively summarized using quantitative graph theoretic measures of network organization (Sporns 2018; Lago-Fernández et al. 2000; Stam and Reijneveld 2007). Thus, using degree centrality, an important graph theoretic measure of network organization (Sporns 2011), it is possible to quantify nodal characteristics.

In a weighted network, a node's degree centrality is computed as the weighted sum of *all* edges connected to it (Rubinov and Sporns 2010); thus, DC captures cumulative relationships between *all* nodes of the network, and the relative value of any given node within that functional structure (Zuo et al. 2012). High degree centrality indicates a node with "dense" functional connections, and consequently a high level of information exchange (Freeman 1977), with the rest of the network (Bullmore and Sporns 2009). Thus, in computing degree centrality, "local" information (i.e., at the level of each node) depends on "global" information (i.e., relative to all other nodes). The ranking of nodes by their degree centrality provides ordinal information that can isolate important nodes in a network (Li et al. 2013; Hagmann et al. 2008).

Here, we used ALE and EDE to derive nodes from fMRI data collected while participants engaged in verbal and visual working memory tasks. The typical *n*-back paradigm was used to collect the verbal working memory data (Bakshi et al. 2011; Casey et al. 1995; Diwadkar et al. 2015) ($n = 28$ participants). A visual *n*-back (from the Human Connectome Project dataset) was used to collect the visual working memory data (Falco et al. 2019) ($n = 182$ participants). As noted, when applied to the *same* data from *each participant,* the ALE and EDE approaches can form two different networks. Each network can be composed of unique nodes,

but these are constricted to the same anatomical region. For each network (derived from the two different approaches), we first computed each node's degree centrality in each network. Estimates of degree centrality were compared between techniques, and we also compared the ranking of network nodes based on this measure. Our results demonstrate that *both* degree centrality and the ranking of network nodes significantly differ between the two networks estimated from the same participants.

Methods

Methods unique to the verbal and visual *n*-back

Participants (verbal *n*-back task)

Twenty-eight healthy individuals provided informed consent, or written assent, to participate in the study (Mean age: 19.25 years; Age range: 17–23 years; 14 males). Participants were recruited through community-based advertisements, and all experimental procedures were approved by the Human Investigative Committee at the Wayne State University School of Medicine.

Participants (visual *n*-back task)

Task-based fMRI scans from a visual working memory task of the HCP database were included to extend investigation of our questions of interest to a parallel working memory domain in a unique (and larger) dataset. Data from 182 participants whose age (22–25 years) most closely matched that of the participants in the verbal *n*-back (17–23 years) were included. All included participants successfully completed the task. Raw HCP fMRI data were downloaded and submitted to the pipeline shown in Fig. 1.

fMRI data collection (verbal *n*-back task)

Functional MRI (fMRI) BOLD-contrast time series data collection was performed using gradient echo planar imaging (EPI) on a 3 T Siemens Verio system using a 12-channel volume head coil (TR: 2.6 s, TE: 29 ms, FOV: 256 × 256 mm^2, acquisition matrix: 128 × 128, 36 axial slices, voxel dimensions: 2 × 2 × 3 mm^3). In addition, a 3D T1-weighted anatomical MRI image was acquired for each participant (TR: 2200 ms, TI: 778 ms, TE: 3 ms, flip angle = 13°, FOV: 256 × 256 mm^2, 256 axial slices of thickness = 1.0 mm, matrix = 256 × 256). A neuroradiologist reviewed all scans to rule out clinically significant abnormalities.

fMRI data collection (visual *n*-back task)

fMRI BOLD-contrast time series data collection was performed using gradient echo EPI on 3 T Siemens "Connectome Skyra" machines with a 32-channel head coil (TR: 720 ms, TE: 33.1 ms, FOV: 208 × 180 mm^2, acquisition matrix: 104 × 90, 72 axial slices, voxel dimensions: 2 × 2 × 2 mm^3). A 3D T1-weighted anatomical MRI image was also acquired for each participant (TR: 2400 ms, TI: 1000 ms, TE: 2.14 ms, flip angle: 8°, FOV: 224 × 224 mm^2).

Task and data preprocessing (verbal *n*-back task)

Participants engaged in a 2-back verbal working memory task (Bakshi et al. 2011; Diwadkar et al. 2017) during which letter stimuli were projected in sequence (Presentation Time: 500 ms; ISI: 2500 ms). Participants signaled (by button press) if the letter was a target letter (0-Back condition), or identical to the one shown two letters previously in the sequence (2-Back condition). A block design was employed with 3 experimental conditions: 0-back (30 s/epoch; 5 epochs), 2-Back (30 s/epoch; 5 epochs) and rest (20 s/epoch; 10 epochs). Extended rest epochs were also included to reduce fatigue.

Task and data preprocessing (visual *n*-back task)

Participants viewed a series of visual stimuli (non-mutilated body parts with no nudity, faces, tools, or places). Each scan had two runs of 8 task blocks (10 trials, 25 s per block) split evenly between the 2-back and 0-back conditions, and 4 resting blocks (15 s). A detailed explanation of the task, as well as visualization of the actual stimuli, is available on the HCP website and other sources (Moeller et al. 2010; Feinberg et al. 2010; Setsompop et al. 2012; Xu et al. 2012).

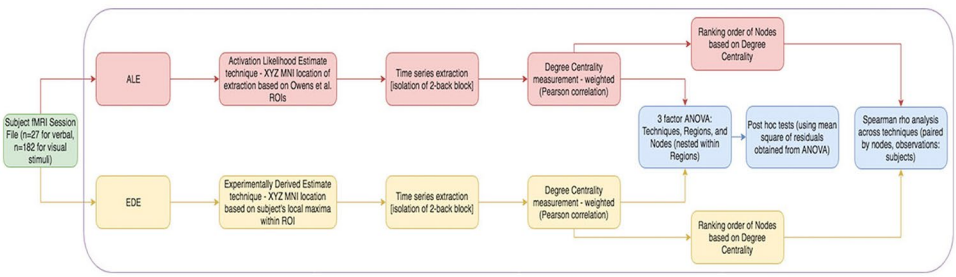

Fig. 1 The depicted flowchart shows the analysis pipeline used for both the verbal and visual *n*-back task analysis

All fMRI BOLD data were processed employing established methods for temporal preprocessing (slice timing correction), followed by spatial preprocessing in SPM8. In spatial preprocessing, the echo planar images were manually oriented to the AC–PC line with the reorientation vector applied across the echo planar image set, realigned to a reference image to correct for head movement, and co-registered to the anatomical high-resolution T_1 image. This high-resolution T_1 image was normalized to the Montreal Neurological Institute (MNI) template, with the resultant deformations subsequently applied to the co-registered EPI images for normalization. Low-frequency components were removed using a low-pass filter (128 s) and images were spatially smoothed using a Gaussian filter [8 mm full-width half-maximum (FWHM)]. An autoregressive (AR) model was used to account for serial correlation, and regressors were modeled as box-car vectors (separately for each of the experimental conditions) were convolved with a canonical hemodynamic reference waveform, with the six motion parameters included in the model as effects of no interest.

Coordinate identification (verbal *n*-back task)

Initial coordinate locations for nodes of the ALE network were compiled from a previously published meta-analysis of 24 unique verbal *n*-back working memory studies (Owen et al. 2005). The BrainMap database is considered the canonical repository for activation peaks (Eickhoff et al. 2012); therefore, in the interests of convergence, these 24 loci were compared to those in the database's repository. Using the Sleuth (Laird et al. 2005) and GingerALE programs in BrainMap, the following search criteria were established to isolate relevant studies: (a) working memory (domain), (b) *n*-back (behavioral task), and (c) letters (visual stimuli). This comparative search identified a total of 66 unique studies, of which 15 met the search criteria (the remaining 51 included diseased cohorts and were excluded).

The BrainMap program found five voxel clusters using the same parameters as Owen et al. ($p_{FDR} < 0.01$, cluster extent > 200 mm^3): four (left inferior Parietal Lobule, BA39; left dorsal Anterior Cingulate Cortex, BA32; left and right lateral Premotor Cortex, BA6) were also reported by Owen et al. (2005). This comparison indicated that the Owen et al. (2005) meta-analysis subsumed the BrainMap nodes, by producing a more comprehensive set of coordinates. Therefore, this set was retained for subsequent exploration and analyses.

These ALE meta-analytic coordinate locations were translated into MNI space (Papademetris et al. 2017), yielding 17 unique cortical, thalamic, and cerebellar loci (Falco et al. 2019). Of these, only 13 could be used here: four loci [right medial Cerebellum, medial Cerebellum, left lateral Cerebellum, and left ventrolateral Prefrontal Cortex (PFC) (BA6)] had to be excluded because their corresponding EDE location of maximal activation was already paired with another ALE location (mapping ALE coordinates to anatomical regions was a pre-requisite for the EDE approach, and analyses were restricted to a *single* maximum in any anatomical region). These thirteen coordinates gave the locations of ALE-defined nodes that were subsequently used to assess network functional connectivity. As noted in the Introduction, this network can be considered a representative working memory network.

The thirteen nodes provided constraints for coordinate identification for the EDE technique. Using Automated Anatomical Labeling (AAL) (Maldjian et al. 2003), a regional label was assigned to each ALE location. Then, EDE coordinates were located at individual-participant activation maxima within each of these labeled locations. Thus, *all* labeled locations within the network were finally assigned one ALE node and one EDE node. The nodes lie within broadly defined cortical regions (Frontal/Cingulate, Motor, Parietal and Subcortical), with different commitments to working memory (Cabeza and Nyberg, 2000). Therefore, each node was given its unique regional assignment (to one of these four regions), and in all subsequent statistical analyses, Region served as a Factor of interest (while Nodes were nested within Regions, See "Degree centrality analysis" for further description).

Coordinate identification (visual *n*-back task)

As with the verbal *n*-back task, the BrainMap database was used to verify the locations of the nine non-verbal working memory clusters identified by the Owen et al. (2005) meta-analysis. Using the database and BrainMap associated programs (Sleuth and GingerALE), the following search criteria were utilized to identify the list of studies from which to perform this localization: (a) working memory (domain), (b) *n*-back (task), (c) any stimulus from the HCP list or within the Owen et al. (2005) non-verbal category. Of the resulting 37 datasets, 27 were discarded because they used atypical cohorts. In the remaining 10 studies, the parameters from Owen et al. (2005; $p_{FDR} < 0.01$, cluster extent > 200 mm^3) were used, but no significant voxel clusters were found. As with the verbal *n*-back task, these preliminary investigations indicated that the Owen et al. (2005) meta-analysis subsumed the coordinates in BrainMap, and, therefore, those nine nodes were considered the representative ALE nodes. These nodes were again used to constrain the search for coordinates in the EDE method, with the entire method replicated (Fig. 1).

Methods common to the verbal and visual *n*-back

Time series extraction

Time series representing the first eigenvariate from the effects of interest contrast ($p < 0.05$) were extracted from

each ALE node (3-mm radius centered around the specifically identified location) for each participant. If the ALE-identified coordinate did not yield a significant activation for a participant, the most proximate supra-threshold peak within a search radius of 10 mm was used. If no activation peak was found within 10 mm, time series for that ALE node was not reported for that participant. As noted earlier, all ALE nodes provided constraints for coordinate identification for the EDE technique. Using Automated Anatomical Labeling (AAL) (Maldjian et al. 2003), a regional label was assigned to each ALE location. Then, EDE coordinates were located at individual-participant activation maxima within each of these labeled locations (3 mm radius centered around the participant-specific significance peak). The application of spatial, anatomical and statistical criteria resulted in a small loss of the available nodes across participants and data sets (verbal *n*-back: 4%, visual *n*-back: 0.03%).

Analyses were restricted to blocks associated with the 2-back (i.e., active working memory) condition. Time series from these blocks were submitted for subsequent connectivity analysis, and the resultant bivariate correlation coefficients permitted the computation of weighted degree centrality (see below).

Degree centrality analysis

For both verbal and visual *n*-back data, weighted degree centrality representing the weighted sum of the edges connected to a node was calculated based on the Pearson correlation coefficient (*r* value). Scripts for the analysis were written in R (Rstudio, 2016), using the "swldf" package to import data and the "psych" package for statistical analysis. The specific steps that went into these calculations are detailed below.

For each participant, a symmetric correlation matrix for each of the ALE and EDE technique was constructed from time series extracted from the appropriate nodes. This resulted in two adjacency matrices per participant. In each matrix, by convention each cell represented an edge within the graph, and the correlation (*r* score) represented the strength of the relation between nodes for that edge. For each participant, degree centrality for each node was obtained by computing the weighted sum of each column in the correlation matrix.

The degree centrality measures were submitted to a three factor, repeated-measures analysis of variance (ANOVA). The factors (all modeled as within-participant's factors) were Technique (ALE vs EDE), Regions (Verbal *n*-back: Frontal/Cingulate, Motor, Parietal, Subcortical; Visual *n*-back: Frontal and Parietal), and Nodes (nested within Regions). Post hoc tests were conducted using the standard error term computed from the mean square of the residuals obtained from the ANOVA (Ruxton and Beauchamp 2008).

Spearman rho (ρ) analysis

The two principal aims of this investigation were to explore the impact of node identification technique on: (1) degree centrality itself, and (2) *rank ordering* of nodes based on their degree centrality (Mones et al. 2012). The explorations from the second aim complement those from the first because: (a) the two techniques could produce different centrality measures for each node and participant, *and yet* (b) their nodal ranking might be identical. In such a case, the impact of each of the techniques would be equivocal. To attempt to reach an unequivocal assessment, we conducted a Spearman ρ analysis to investigate whether in each participant, the ordinal ranking of nodes (based on their degree centrality) differed between techniques.

An R script was written to execute this second aim. The nodes in the networks produced by each of the two techniques were first ranked in ascending order of degree centrality (resulting in rankings from 1 to 13 for the verbal *n*-back, and 1–9 for the visual *n*-back). Then, for each participant, these ranks were analyzed with a Spearman's ρ test. The results of these analyses allowed us to assign individual participants in each of the working memory datasets into "Correlated" (i.e., the median ranking of nodes of the two networks was similar) and "Uncorrelated" (i.e., the median ranking of nodes of the two networks was not correlated) groups.

Results

Results are reported in the order of task, with the verbal *n*-back results followed by those from the visual *n*-back. Within each section, we first report the results of the ANOVA (relating to differences in degree centrality) and then of the Spearman's ρ analysis (relating to differences in node ordering). Results from the ANOVA show significant main effects and interactions (unpacked using subsequent post hoc pairwise tests). *Particularly relevant for our investigation were potential interactions between the factors of Technique and Node*s (nested within Regions). Significant effects are pictorially depicted for the verbal *n*-back task (Figs. 2 and 3) and the visual *n*-back task (Figs. 5 and 6). As noted (Methods), results from the Spearman's ρ analysis permitted assignment of participants into correlated and uncorrelated sub-groups. Any differences between the ordering in each of the sub-groups are summarized in the form of radial plots and heat maps for the verbal *n*-back (Fig. 4) and visual *n*-back (Fig. 7) task.

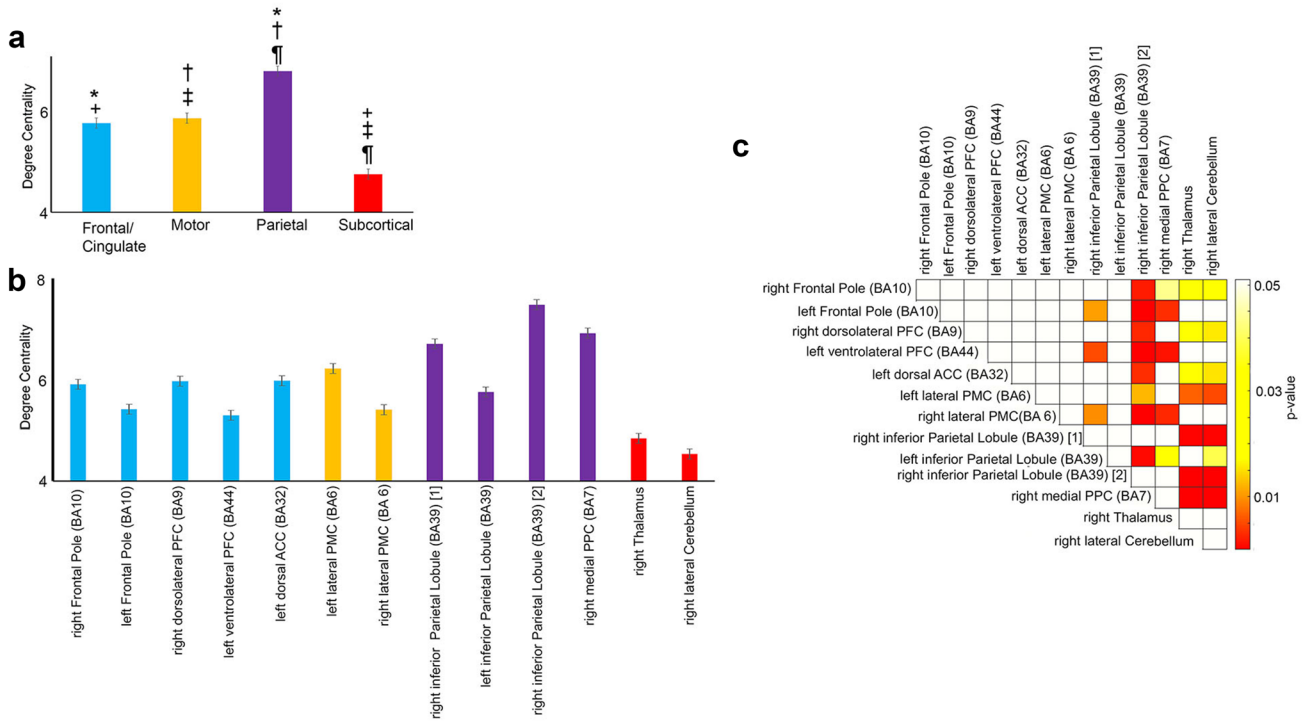

Fig. 2 **a** Mean degree centrality is depicted at the regional level (Frontal/Cingulate, Motor, Parietal and Subcortical) to highlight the main effect of Region. Pairwise significant differences are depicted using the symbols above the bars. **b** Mean degree centrality for each of the 13 nodes organized in the Anterior to Posterior axis is depicted to highlight the main effect of Nodes (nested within Regions). Color schemes for depicting nodes are maintained in all subsequent figures. **c** Pair-wise differences associated with the main effect in (**b**) were unpacked using the ANOVA residuals and corresponding post hoc tests (see "Methods"), with the results depicted in the heat map. As one can observe from **c**, most of the significant interactions occur between nodes paired with Parietal or Subcortical nodes. All error bars for (**a**, **b**) come from the standard error associated with the residuals obtained from the ANOVA

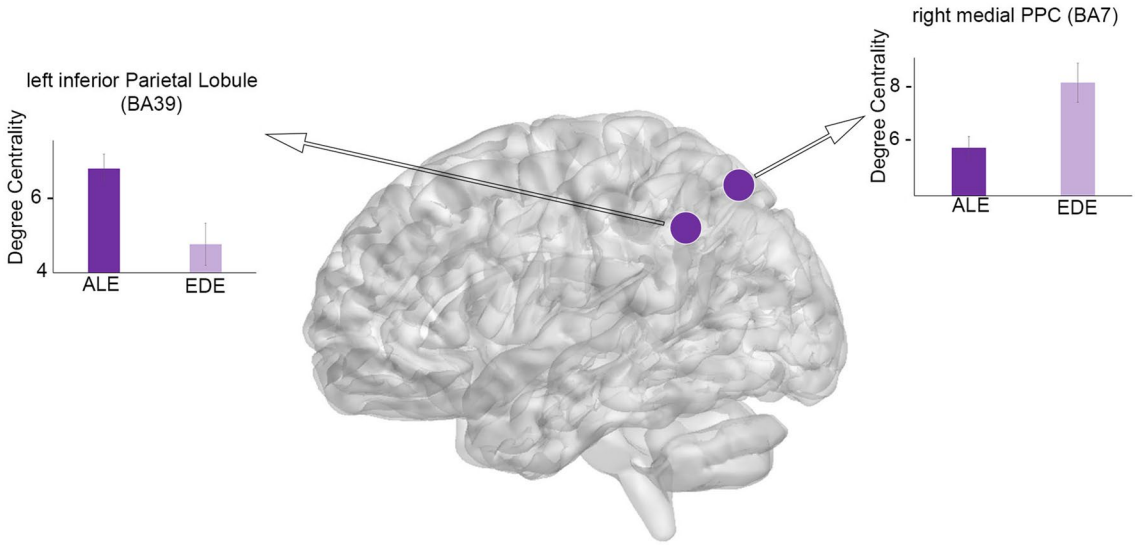

Fig. 3 The three-way ANOVA found a significant interaction between techniques and nodes. The Techniques x Nodes (nested within regions) interaction revealed technique-related effects (ALE vs. EDE) on the degree centrality of two nodes, the right medial PPC and the left inferior parietal lobule. These effects are depicted in the adjoining bar graphs (error bars are derived from the standard error associated with residuals obtained from the ANOVA). For the right medial PPC, degree centrality was higher when nodes were identified using the EDE technique

Verbal *n*-back task

Degree centrality analysis

The three-way nested analysis of variance revealed two significant main effects. We observed a main effect of Region ($F_{3,645} = 12.8$, $p < 0.001$, MSe = 83.58) and Nodes (nested within Region) ($F_{9,645} = 2.16$, $p = 0.023$, MSe = 14.07). The main effect of Region is depicted in Fig. 2a (significant inter-pair differences are denoted by paired symbols, $p < 0.05$). The parietal region was characterized by the highest degree centrality and post hoc tests showed that both the Subcortical and Parietal regions were significantly different from the other regions. Figure 2b shows the mean degree centrality for each node (where nodes are organized by region), and to facilitate easy access to all significant pair-wise comparisons, the heat map in Fig. 2c depicts probabilities for any significant pair-wise differences in degree centrality. As seen, the sub-cortical nodes (thalamus and lateral cerebellum), the right medial posterior parietal cortex (PPC), and the right inferior parietal lobule evinced widespread differences in degree centrality compared to other nodes.

Of particular relevance for our investigation was the Technique x Nodes (nested within Regions) interaction. Indeed, the ANOVA revealed this interaction to be highly significant ($F_{9,645} = 2.6$, $p = 0.006$, MSe = 16.95). Post hoc analyses were employed to identify the specific nodes for which degree centrality was significantly different based on the two techniques. As seen in Fig. 3, these nodes were the left inferior Parietal Lobule, and the right medial PPC. Given the relevance of these regions for working memory processing, these effects must be considered highly salient.

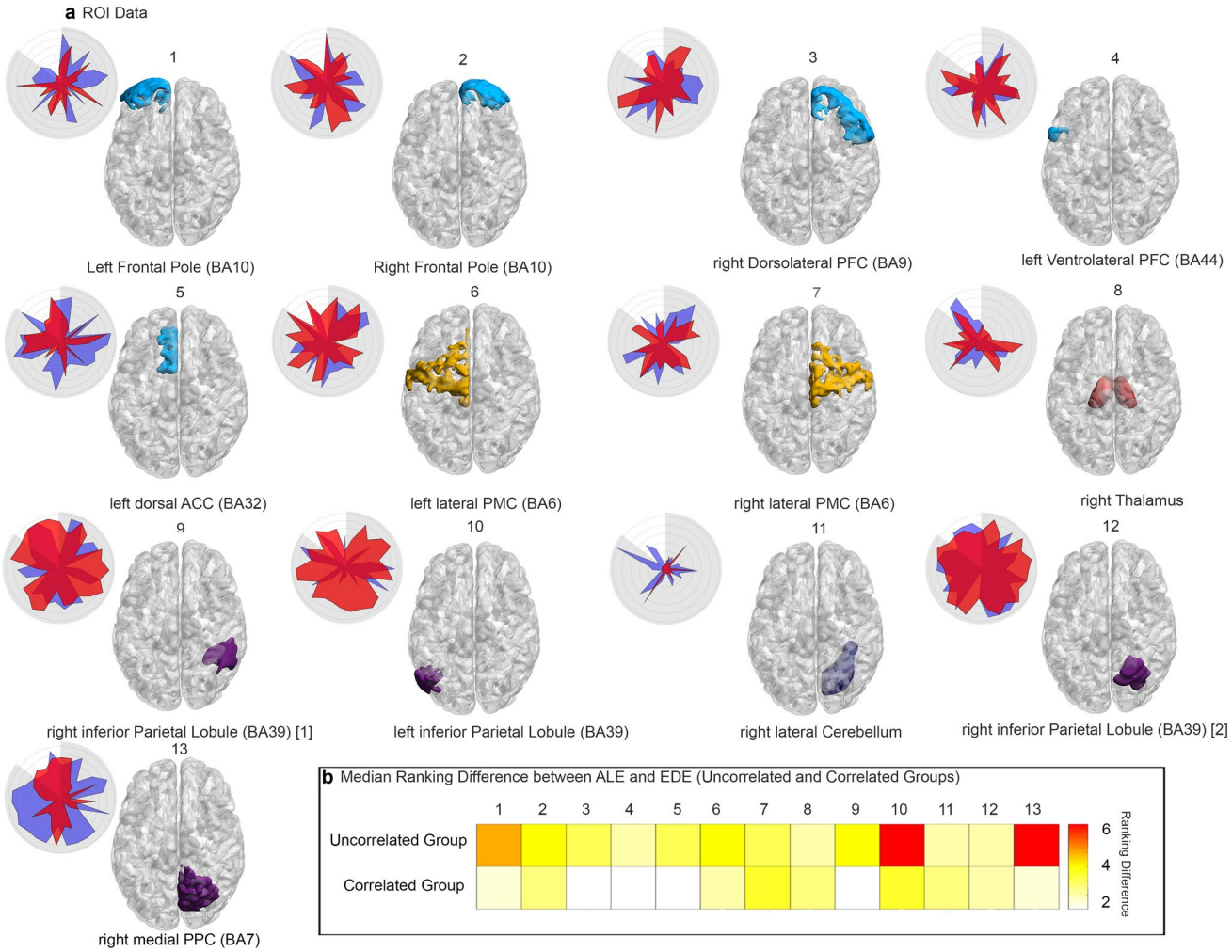

Fig. 4 **a** To represent results from the Spearman ρ analysis, radial plots are displayed for each node. Within each, the amplitude represents *each* individual participant's estimated node rank from each technique (red = ALE, blue = EDE). Shaded portions of the radial plots represent the individuals that were found to have uncorrelated ranks across all nodes (85% of all participants). **b** The median difference in rank across techniques for the uncorrelated and correlated participants is plotted as a heat map

Spearman ρ analysis

The Spearman ρ analysis found that only 4 participants (15%), showed correlated node rankings between techniques. Thus, for the majority (85%), node rankings between the ALE and EDE techniques were uncorrelated. To emphasize the importance of these effects, it is essential to present the data efficiently across *all* participants. Therefore, we employed radial plots for each region of interest (Fig. 4a). In each plot, the amplitude at each point represents the estimated node rank for *each* participant and Technique. Linking these points results in ALE-related (Red) and EDE-related (Blue) curves. Had both techniques resulted in largely correlated ranks across all nodes and for all participants, the curves for ALE (Red) and EDE (Blue) would be overlapping. However, the observed effects across participants belie such overlap. The shaded area, denoting participants (85% of the group) with uncorrelated ranks, indicates that the overlap in curves is highly variable. The adjoining heat map (Fig. 4b) summarizes this effect. The colors in the map code for the median difference in ranking between the ALE and EDE techniques for the uncorrelated participants and correlated participants (warmer colors reflect greater differences). Expectedly, the difference is higher for the uncorrelated group (top row).

Visual *n*-back

Degree centrality analysis

Two significant main effects were observed in the three-way nested analysis of variance. We observed a main effect of Techniques ($F_{1,3257} = 105.15$, $p < 0.001$, MSe = 287.28) and Nodes (nested within Regions; $F_{7,3257} = 10.17$, $p < 0.001$, MSe = 27.03). These results are visually explored in Fig. 5 (which maintains the structure of Fig. 3). Figure 5a unpacks the main effect of Techniques, while 5b depicts the main effect of Nodes (nested within regions). The probability heat map seen in 5c is an extension of 5b and depicts all significant pairwise differences between nodes.

As seen in 5a, the main effect of technique was driven by higher degree centrality observed in the EDE technique.

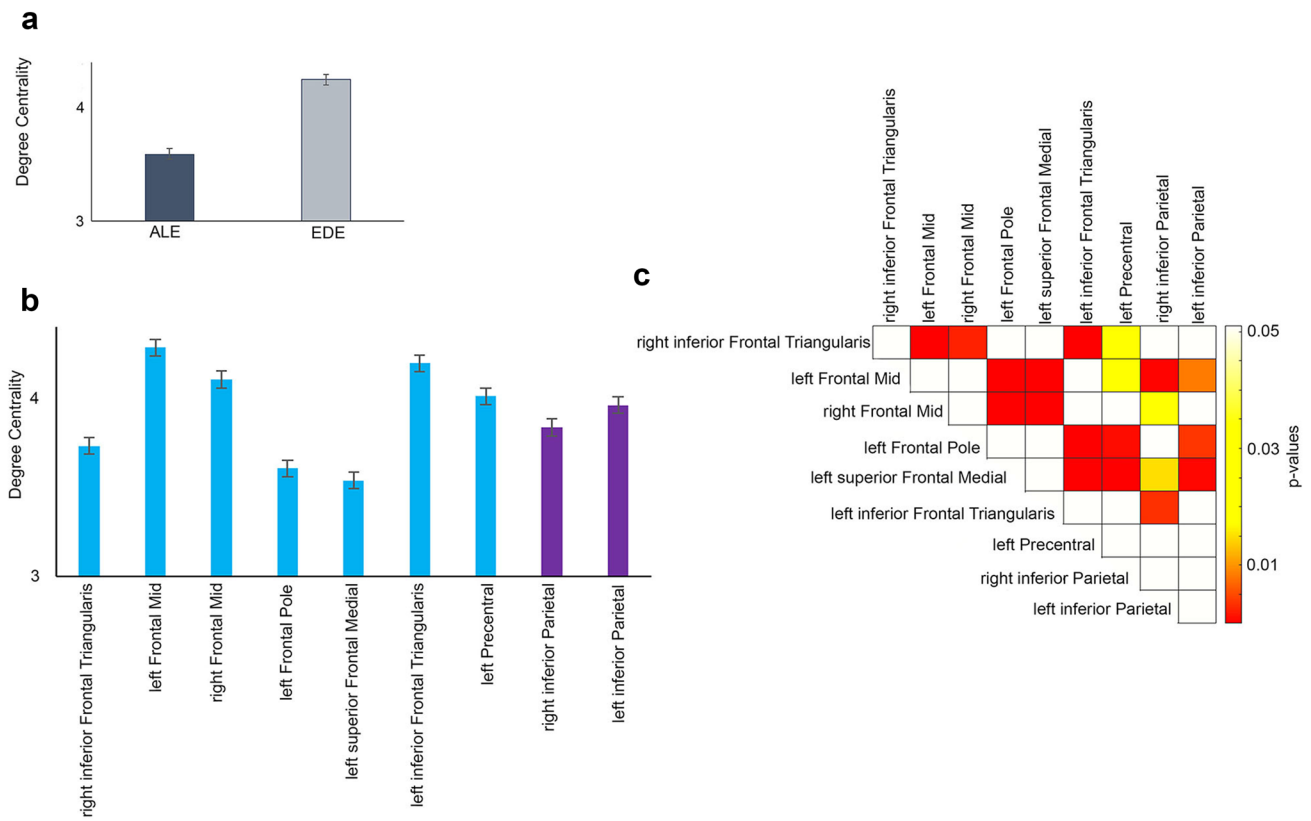

Fig. 5 The figure depicts results of the ANOVA and highlights the significant main effects for Techniques and Nodes (nested in regions) for data from the visual n back task. **a** The mean estimated degree centrality is depicted for each of the ALE and EDE techniques. **b** The degree centrality estimates from the nine nodes across the Frontal and Parietal Regions are depicted. All error bars are derived from the standard error associated with the residuals obtained from the ANOVA. **c** Pair-wise differences associated with the main effect in (**b**) were unpacked using the ANOVA residuals and corresponding post hoc tests, with the results depicted in the heat map

Figure 5b shows that the node with the highest estimated degree centrality was the left Mid-Frontal Cortex. As seen in the heat map (5c), the left Frontal Mid and the left superior Frontal Medial (left superior Medial-Frontal Cortex) nodes differed the most from other nodes.

As with the verbal *n*-back task, analyses of the visual *n*-back also revealed a highly significant Technique x Nodes interaction ($F_{7,\ 3257} = 23.75$, $p < 0.001$, MSe = 64.88). Post hoc analyses were used to discover the specific nodes driving the interaction term. These seven nodes are depicted in Fig. 6. In six, degree centrality estimated based on the EDE technique was higher than ALE.

Spearman ρ analysis

The Spearman ρ analysis found that only 14 participants (8%) showed correlated node rankings across techniques. Thus, as with the verbal *n*-back task, for the majority (92%) node rankings were uncorrelated across techniques. Figure 7 (which emulates Fig. 4), efficiently depicts all participant data for each of the nine nodes using radial plots. The subgroup with uncorrelated ranks is denoted by the shaded area and (as with Fig. 4) the overlap in curves is highly variable. The adjoining heat map (Fig. 7b) summarizes this effect by displaying the median difference in rank between the ALE and EDE techniques for the uncorrelated and the correlated participants (again, the median difference is higher for the uncorrelated group, top row).

Evaluating the role of Euclidean distance between ALE and EDE nodes

These results implicate differences in node identification techniques as driving differences between measures of network function. However, corresponding nodes identified by each of the ALE and EDE techniques are separated by quantifiable Euclidean distances, and it is plausible that the magnitude of the Euclidean distance might mediate estimates of (and differences between estimates of) Degree Centrality and node ranking. Nodes that are closer together in space may fall within the same resolution element (post smoothing), have more similar time courses, and effectively have more similar profiles within networks. Were such to be the case, inter-technique differences in node centrality or rank order would simply be an emergent property of physical differences in node location rather than technique-specific effects.

These concerns motivated investigation of the role of Euclidean Distance (*D*) between each of the corresponding ALE and EDE coordinates in capturing any variation in

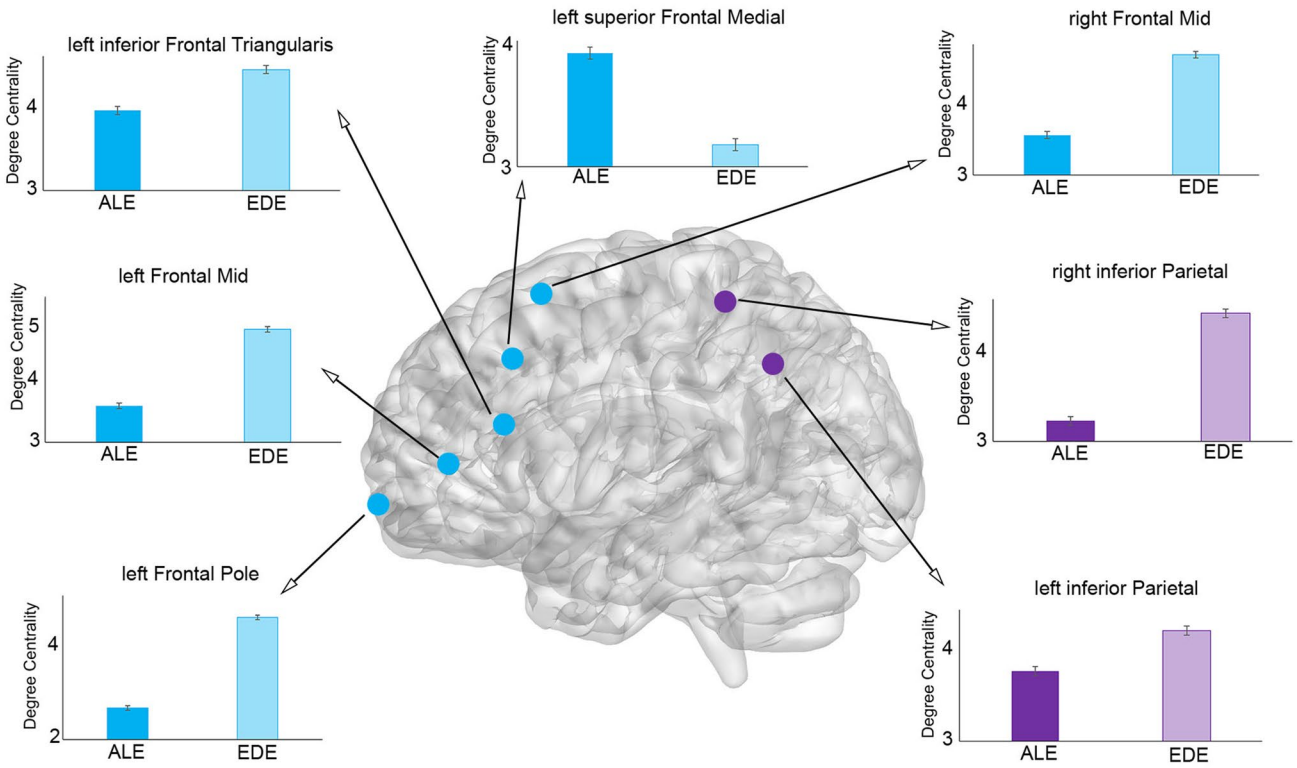

Fig. 6 The result from the visual n-back task shows the seven nodes with significantly different degree centralities between the two techniques. In six of the seven, higher degree centralities were observed in the EDE technique compared to ALE technique

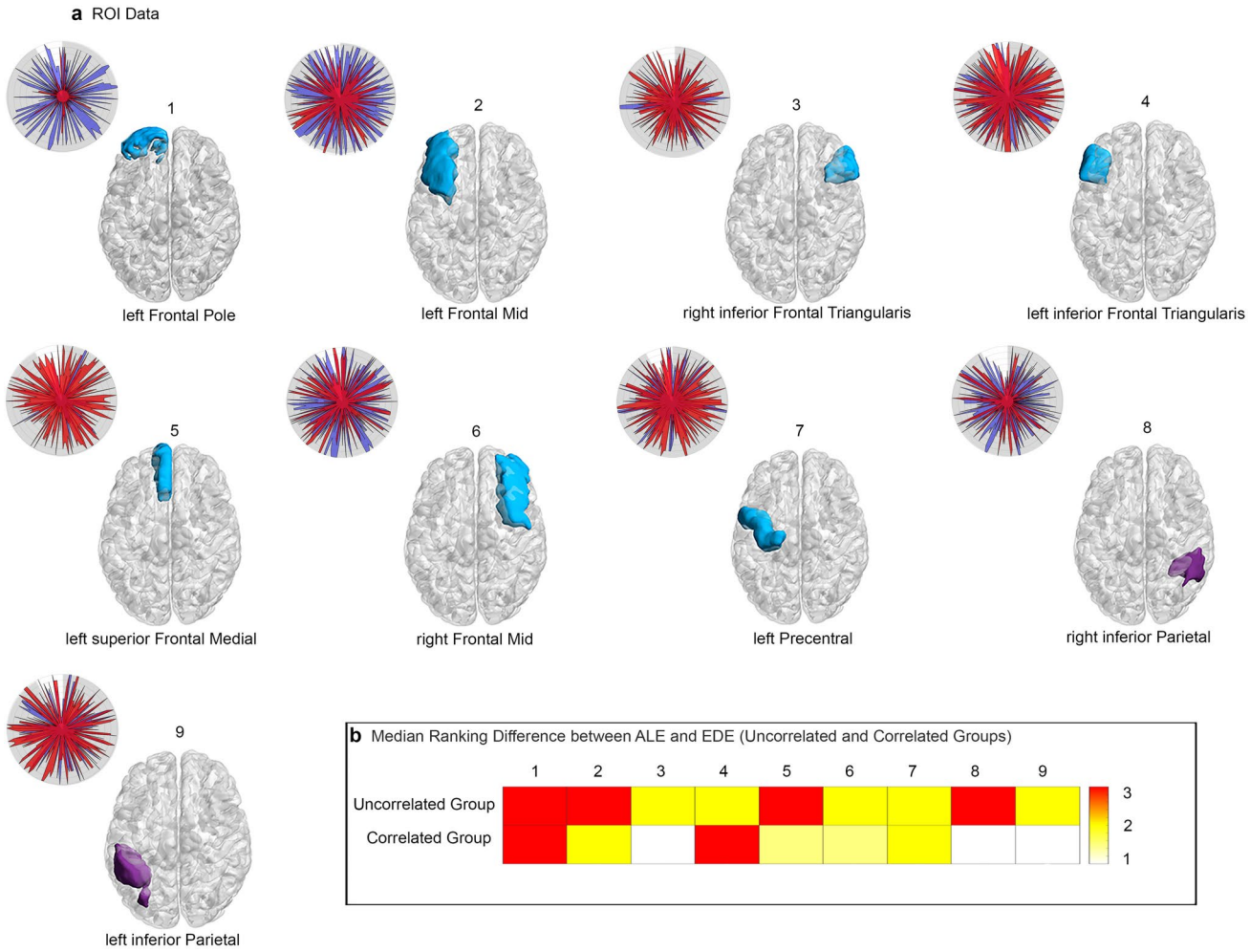

Fig. 7 Radial plots depict data from the visual n-back (the conventions are maintained from Fig. 4, red = ALE, blue = EDE). **a** The shaded portion for the visual n-bask task represents the 92% of the group's participants who were found to have uncorrelated rankings between techniques. **b** As in Fig. 4b, the median difference in rank across techniques for all uncorrelated and correlated participants is visualized as a heat map with the median ranking difference seen as higher in the uncorrelated group (top row)

the differences between Degree Centrality and node ranking. First, Euclidean distance was calculated in coordinate space:

$$D = \sqrt{\left(x_{\mathrm{ALE}} - x_{\mathrm{EDE}}\right)^2 + \left(y_{\mathrm{ALE}} - y_{\mathrm{EDE}}\right)^2 + \left(z_{\mathrm{ALE}} - z_{\mathrm{EDE}}\right)^2}.$$

Next, using linear regression models (with D as the predictor variable), we estimated the degree of variance in the difference in Degree Centrality or node ranking accounted for by Euclidean distance. Four additional analyses were conducted (two each for the verbal and visual working memory tasks). Because of the amount of data (i.e., all nodes across all participants were entered in each of the four models), we were interested in capturing the degree of variance accounted for by Euclidean distance for each difference metric (the models were overpowered for correlational analyses).

For the verbal n-back task (Supplementary Fig. 1a), Euclidean distance (D) explained only 1.3% of the variance ($r^2 = 0.013$) relating to differences in Degree Centrality, revealing a very small effect ($\beta = 0.016$), and only 0.1% of the variance ($r^2 = 0.001$) relating to differences in nodal ranking (again with a very small effect, $\beta = 0.012$). The effects for the visual n-back (Supplementary Fig. 1b) were similarly miniscule. Here, Euclidean distance (D) explained only 2.6% of the variance ($r^2 = 0.026$) relating to differences in Degree Centrality, with a very small effect ($\beta = 0.012$), and only 5.5% of the variance ($r^2 = 0.055$) relating to differences in nodal ranking ($\beta = 0.03$).

Evaluating participant-specific networks

Nodes identified using the ALE technique reflect data aggregation across studies (and participants), whereas nodes

identified using the EDE technique are tuned to individual differences in activation maxima (albeit in anatomical ROIs defined by ALE) *and for the specific condition of interest* (2-back). Further analyses were initiated to evaluate whether participant-specificity alone was a *sufficient condition* for generating increases in estimated Degree Centrality associated with the EDE technique. First, participant-specific nodes were identified in the ALE-defined anatomical ROIs of interest, but all local activation maxima were isolated using the 0-back (rather than the 2-back) condition, with time series extracted from these individualized peaks (see "Time series extraction"). This EDE-related technique (henceforth EDE_0) retains the property of participant-specificity, but subsequent characterization of time series was restricted to the vector onsets for the 2-back conditions (thus, EDE_0 did not retain *condition*-specificity).

The structure of the subsequent statistical analyses replicated what was previously conducted ("Degree centrality analysis"), but the factor for Technique now consisted of three conditions: ALE, EDE_2 (previously EDE) and EDE_0. Here, EDE_2 and EDE_0 retain participant-specificity, but only EDE_2 retains participant- *and* condition-specificity. The focus of these analyses was the main effect of Technique (see Supplementary Data for a full reporting of the results).

For the verbal *n*-back task, the main effect of Technique was highly significant ($F_{2,860} = 88.33$, $p < 0.001$, MSe = 542.99). As seen in Supplementary Fig. 2a, Degree Centrality for EDE_2 and ALE were comparable (as in the original analyses), and both were significantly greater than EDE_0. The main effect of Technique was also highly significant for the visual *n*-back task ($F_{2,4844} = 74.17$, $p < 0.001$, MSe = 190.12). As seen in Supplementary Fig. 2b, EDE_2 was significantly greater than both ALE (as in the original analyses) and EDE_0.

These results indicate that the EDE_2 technique which was *both* participant- *and* condition-specific gave equivalent or higher estimates of Degree Centrality than ALE, and higher estimates than the participant-specific EDE_0. Thus, participant-specificity appeared to *not be* a sufficient condition, but rather participant- *and* condition-specificity are required attributes for this effect.

Discussion

The primary aim of this investigation was to compare the effects of different node identification techniques (ALE and EDE) on estimates of degree centrality of network nodes in verbal and visual *n*-back task conditions. A related secondary aim assessed whether the ALE and EDE techniques also resulted in different rankings of nodes based on their degree centrality estimates. In the primary analyses, our most salient result was revealed by significant interaction terms [Techniques × Nodes(Regions)] in the three-way ANOVA. These effects indicated that the choice of node identification technique (ALE or EDE) exerted a significant effect on estimates of degree centrality for both the verbal (Fig. 3) and visual (Fig. 6) *n*-back tasks. We also observed main effects of technique (EDE > ALE) for the visual *n*-back task (Fig. 5a). We presented evidence that choice of node identification technique exerted effects at the level of the participant, resulting in uncorrelated node orders in the majority of participants for both the verbal (Fig. 4) and visual (Fig. 7) *n*-back tasks. Finally, additional evaluation indicated that these effects were only weakly related to the Euclidean Distance between corresponding ALE and EDE nodes (Supplementary Fig. 1), and were strongly related to the participant- *and* condition-specific aspects of EDE (Supplementary Fig. 2). We emphasize that the focus of the investigation was *not* to study the architecture of working memory. Rather, working memory was used because it is a robustly understood behavioral domain for which fMRI data can be tractably collected, and with publicly available large data sets. Coupled with graph theoretic measures, access to complementary data sets allowed us to quantify the *difference* between the two node identification techniques.

Techniques (ALE vs. EDE) exert effects on degree centrality at the level of nodes

Unpacking the interaction terms in Fig. 3 (verbal *n*-back) and Fig. 6 (visual *n*-back) illustrated the fact that the ALE and EDE techniques resulted in networks with different degree centrality estimates for *specific nodes*. For the verbal *n*-back task (Fig. 3), these effects were observed for the two parietal nodes. For the visual *n*-back task (Fig. 6), these effects were more general, observed in five frontal nodes and the same two parietal nodes. In our analyses (and the majority of published studies), centrality estimates were derived from measures of undirected functional connectivity (see "Methods"), using bivariate correlation models. These effects suggest that EDE-derived networks have a higher mean correlation coefficient across all edges than ALE-derived networks. Indeed, additional analyses indicated this to be true for both the verbal *n*-back task (mean $r_{ALE} = 0.46$ vs. mean $r_{EDE} = 0.48$, $p = 0.05$), and the visual *n*-back task (mean $r_{ALE} = 0.45$ vs. mean $r_{EDE} = 0.53$, $p < 0.0001$). This significant difference along with the previously noted Technique x Nodes interaction suggests that each technique provides different estimates of local characteristics of the network's nodes. Thus, even though the identification of nodes by ALE and EDE techniques was restricted to *the same anatomical region*, the EDE technique (*which is sensitive to both individual differences in activation maxima and condition-specificity*) discovered networks with significantly higher synchrony.

Effects of regions and nodes

The structure of the analysis also permitted discovery of differences in estimates of degree centrality *independent* of technique. As seen in Fig. 2a, for the verbal *n*-back task, the parietal region was characterized by the highest degree centrality, whereas the sub-cortical region was characterized by the lowest degree centrality. These effects were driven in part by two nodes (Fig. 2b, c): the right medial PPC (BA7) and left inferior Parietal Lobule (BA39). While, our aims were not to study working memory per se, these findings nevertheless emphasize the centrality of the inferior parietal lobule in this domain, with multiple studies associating it with the maintenance and updating of memoranda (Borst and Anderson 2013). The patterns observed for the visual *n*-back task (Fig. 5b) were different, not involving the inferior parietal lobule. Rather, frontal nodes (left Mid-Frontal Cortex and left inferior Frontal Triangularis) emerged as having the highest estimates of degree centrality, and internode differences (Fig. 5c). Regardless of the possibility that modality-specific and sample-size effects might modulate estimates of degree centrality, these analyses highlight the importance of frontal and parietal regions and their interactions for working memory (Ravizza et al. 2004; Mehta et al. 2000; Baldo and Dronkers 2006).

Quantifying effects at the level of individual participants

A more intriguing set of results emerged when comparing the rank ordering of nodes by their centrality within the set of participants in each task. This ordering was different between the ALE and EDE techniques in the majority of participants. The ranking of nodes by degree centrality is used in the field of topology to measure a node's importance in a biological network (Cadini et al. 2009). A high degree centrality measure implies a high rate of information exchange with other nodes in the network. Thus, the measure can be used to rank nodes in terms of their relative importance (Pavlopoulos et al. 2011). In this regard, Figs. 4 and 7 are particularly salient because (unlike data summarized over participants) they present data from *all* participants in *each* data set. As these analyses show, 85% of the participants in the verbal *n*-back task and 92% of the participants in the visual *n*-back task, had uncorrelated node order rankings between techniques. For the verbal *n*-back task (Fig. 4), the nodes with the highest median difference in ranking were in the Left Frontal Pole (BA10), left inferior Parietal Lobule (BA39), and right medial PPC (BA7). For the visual n-back task (Fig. 7), the nodes with the highest median difference in ranking were in the left Frontal Pole, left Mid-Frontal Cortex, left superior Medial-Frontal Cortex, and right inferior Parietal Cortex. As noted above, the EDE technique is sensitive to both individual differences in activation maxima and condition-specific effects, exerting an effect on the average degree centrality (see "Techniques (ALE vs. EDE) exert effects on degree centrality at the level of nodes" above), whereas the ALE technique by its nature, cannot be.

General (ALE) and individual-specific networks (EDE)

An implicit question that motivates these analyses is the role of individual differences in identifying networks for subsequent discovery, and whether sensitivity to individual differences impacts the process of discovery. Previous work (Falco et al. 2019) indicated that individual-specific brain networks *are* characterized by different edge strengths between nodes (compared to general and fixed brain networks). Since our ALE locations were explicitly derived from a meta-analysis using working memory tasks, all nodes identified using ALE-based meta-analyses were by definition deemed central to working memory (or any other task-variable being considered). However, the notion that brain *networks* are "fixed" across participants rests on the assumption that *all* nodes' respective time series represent functional information that is *most likely* to be representative across participants. This assumption is separate from the aims of ALE and is likely to be untenable.

The distinction between the individual and the group is characteristic of all biological analyses, and several fMRI studies have pointedly characterized these effects. Resting-state fMRI analyses have indicated that individual variability across the association cortex impacts functional connectivity estimates (Mueller et al. 2013), raising the concern that differences could be amplified in the context of task-activated fMRI (Gordon et al. 2017). Indeed, task-based functional connectivity measures tend to have low similarity across individuals (Gratton et al. 2018), evidence of a high degree of individual variability in estimates of brain *network* organization.

Our analyses also indicate that these effects do not disappear simply by relying on large data sets. In fact, the effects of technique were *more pronounced* for the larger of the two data sets (i.e., the visual *n*-back task). Whereas only 15% of the nodes in the verbal *n*-back task ($n = 28$) were significantly different under the Technique x Node interaction term, fully 78% were different in the visual *n*-back task ($n = 182$). Similarly, the larger data set also revealed a higher percentage of participants (92% vs 85%) with uncorrelated node ranks.

In a final set of investigations, we demonstrated that the advantages enjoyed by the EDE (labeled EDE_2 in the additional analyses) over ALE were not related to the physical distance between EDE and ALE peaks (see Supplementary Fig. 1). Rather, these advantages appeared related to both the participant- and condition-specificity of the technique

(Supplementary Fig. 2). These sets of results further emphasize the importance of incorporating individual variations in the identification of nodes for network analyses.

Conclusions

Functional connectivity analyses typically require investigators to identify nodes used to construct a priori networks for connectivity analyses; this choice has crucial consequences because network attributes are related to the choice of nodes (Butts 2009). The current results extend the effects of previous investigations that showed such choices exerted effects on the graph edges (Falco et al. 2019). Here, we focussed on assessments of local network connectivity, that is the graph vertices (nodes). As we show, a priori choices for node identification exert effects at both the group level and the level of individual participants, as well as on estimates of local network organization. The strength of our results is buttressed by the within-participants design of all the analyses, and the fact that they were conducted in two separate domains of working memory, one with a large dataset.

Publicly available fMRI data sets continue to be published, but "big data" in and of itself *cannot* address the fundamental questions raised by our emerging knowledge of brain function. Techniques such as ALE can indeed reduce uncertainty in activation loci across studies within the same domain, because the technique explicitly incorporates individual (and study-related) variability in reported activation loci. *But,* these loci are themselves averaged across participants within each study. They, thus, "conceal" measures of brain network connectivity, and their modulation by task (Morris et al. 2018). Connectivity measures can only be derived from *individual* time series data, and are themselves estimates (Silverstein et al. 2016). Thus, the relatively greater sensitivity of the hybrid EDE method in exerting effects on graph theoretic measures is perhaps unsurprising.

In the context of fMRI data, we suggest that data aggregation (exemplified by the ALE technique), when used in the service of functional connectivity and in conjunction with graph theoretic analyses, can effectively reduce the ROI search space. However, they may not be useful to prescribe *specific* nodes for further analyses. In this way, the power of big data (i.e., having large participant numbers across many studies) might be used to harness understanding of individual differences in brain network function.

Acknowledgements Preparation of this work was supported by the Charles H. Gershenson Distinguished Faculty Fellowship from Wayne State University, the Lyckaki-Young Fund from the State of Michigan, the Prechter Family Bipolar Foundation, the Children's Hospital of Michigan Foundation, the Children's Research Center of Michigan, the Cohen Neuroscience Endowment, the Dorsey Neuroscience Endowment, and the National Institute of Mental Health (MH 59299).

References

Bakshi N, Pruitt P, Radwan J, Keshavan MS, Rajan U, Zajac-Benitez C, Diwadkar VA (2011) Inefficiently increased anterior cingulate modulation of cortical systems during working memory in young offspring of schizophrenia patients. J Psychiatr Res 45(8):1067–1076. https://doi.org/10.1016/j.jpsychires.2011.01.002

Baldo JV, Dronkers NF (2006) The role of inferior parietal and inferior frontal cortex in working memory. Neuropsychology 20(5):529–538. https://doi.org/10.1037/0894-4105.20.5.529

Borst JP, Anderson JR (2013) Using model-based functional MRI to locate working memory updates and declarative memory retrievals in the fronto-parietal network. Proc Natl Acad Sci USA 110(5):1628–1633. https://doi.org/10.1073/pnas.1221572110

Bressler SL (2002) Understanding cognition through large-scale cortical networks. Curr Dir Psych Sci 11(2):58–61. https://doi.org/10.1111/1467-8721.00168

Bullmore E, Sporns O (2009) Complex brain networks: graph theoretical analysis of structural and functional systems. Nat Rev Neurosci 10(3):186–198. https://doi.org/10.1038/nrn2575

Butts CT (2009) Revisiting the foundations of network analysis. Science 325(5939):414–416. https://doi.org/10.1126/science.1171022

Cabeza R, Nyberg L (2000) Neural bases of learning and memory: functional neuroimaging evidence. Curr Opin Neurol 13(4):415–421. https://doi.org/10.1097/00019052-200008000-00008

Cadini F, Zio E, Petrescu CA (2009) Using centrality measures to rank the importance of the components of a complex network infrastructure. In: Setola R, Geretshuber S (eds) Critical information infrastructure security. CRITIS 2008. Lecture notes in computer science, vol 5508. Springer, Berlin

Casey BJ, Cohen JD, Jezzard P, Turner R, Noll DC, Trainor RJ, Rapoport JL (1995) Activation of prefrontal cortex in children during a nonspatial working memory task with functional MRI. Neuroimage 2(3):221–229. https://doi.org/10.1006/nimg.1995.1029

Diwadkar VA, Burgess A, Hong E, Rix C, Arnold PD, Hanna GL, Rosenberg DR (2015) Dysfunctional activation and brain network profiles in youth with obsessive-compulsive disorder: a focus on the dorsal anterior cingulate during working memory. Front Hum Neurosci 9:149. https://doi.org/10.3389/fnhum.2015.00149

Diwadkar VA, Asemi A, Burgess A, Chowdury A, Bressler SL (2017) Potentiation of motor sub-networks for motor control but not working memory: Interaction of dACC and SMA revealed by resting-state directed functional connectivity. PLoS ONE 12(3):e0172531. https://doi.org/10.1371/journal.pone.0172531

Eickhoff SB, Bzdok D, Laird AR, Kurth F, Fox PT (2012) Activation likelihood estimation meta-analysis revisited. Neuroimage 59(3):2349–2361. https://doi.org/10.1016/j.neuroimage.2011.09.017

Falco D, Chowdury A, Rosenberg DR, Diwadkar VA, Bressler SL (2019) From nodes to networks: How methods for defining nodes influence inferences regarding network interactions. Hum Brain Mapp 40(5):1458–1469. https://doi.org/10.1002/hbm.24459

Feinberg DA, Moeller S, Smith SM, Auerbach E, Ramanna S, Gunther M, Yacoub E (2010) Multiplexed echo planar imaging for subsecond whole brain FMRI and fast diffusion imaging. PLoS ONE 5(12):e15710. https://doi.org/10.1371/journal.pone.0015710

Finn ES, Shen X, Scheinost D, Rosenberg MD, Huang J, Chun MM, Constable RT (2015) Functional connectome fingerprinting: identifying individuals using patterns of brain connectivity. Nat Neurosci 18(11):1664–1671. https://doi.org/10.1038/nn.4135

Freeman L (1977) A set of measures of centrality based on betweenness. Sociometry 40(1):35–41. https://doi.org/10.2307/3033543

Friston K (2003) Learning and inference in the brain. Neural Netw 16(9):1325–1352. https://doi.org/10.1016/j.neunet.2003.06.005

Genon S, Reid A, Langner R, Amunts K, Eickhoff SB (2018) How to characterize the function of a brain region. Trends Cogn Sci 22(4):350–364. https://doi.org/10.1016/j.tics.2018.01.010

Gordon EM, Laumann TO, Adeyemo B, Petersen SE (2017) Individual variability of the system-level organization of the human brain. Cereb Cortex 27(1):386–399. https://doi.org/10.1093/cercor/bhv239

Gratton C, Laumann TO, Nielsen AN, Greene DJ, Gordon EM, Gilmore AW, Petersen SE (2018) Functional brain networks are dominated by stable group and individual factors. Not Cogn Daily Var Neuron 98(2):439–452.e435. https://doi.org/10.1016/j.neuron.2018.03.035

Hagmann P, Cammoun L, Gigandet X, Meuli R, Honey CJ, Wedeen VJ, Sporns O (2008) Mapping the structural core of human cerebral cortex. PLoS Biol 6(7):e159. https://doi.org/10.1371/journal.pbio.0060159

Lago-Fernández LF, Huerta R, Corbacho F, Sigüenza JA (2000) Fast response and temporal coherent oscillations in small-world networks. Phys Rev Lett 84(12):2758–2761. https://doi.org/10.1103/PhysRevLett.84.2758

Laird AR, Lancaster JL, Fox PT (2005) BrainMap: the social evolution of a human brain mapping database. Neuroinformatics 3(1):65–78

Langner R, Rottschy C, Laird AR, Fox PT, Eickhoff SB (2014) Meta-analytic connectivity modeling revisited: controlling for activation base rates. Neuroimage 99:559–570. https://doi.org/10.1016/j.neuroimage.2014.06.007

Li L, Hu X, Preuss TM, Glasser MF, Damen FW, Qiu Y, Rilling J (2013) Mapping putative hubs in human, chimpanzee and rhesus macaque connectomes via diffusion tractography. Neuroimage 80:462–474. https://doi.org/10.1016/j.neuroimage.2013.04.024

Maldjian JA, Laurienti PJ, Kraft RA, Burdette JH (2003) An automated method for neuroanatomic and cytoarchitectonic atlas-based interrogation of fMRI data sets. Neuroimage 19(3):1233–1239

Mancuso L, Costa T, Nani A, Manuello J, Liloia D, Gelmini G, Cauda F (2019) The homotopic connectivity of the functional brain: a meta-analytic approach. Sci Rep 9(1):3346. https://doi.org/10.1038/s41598-019-40188-3

Mehta MA, Owen AM, Sahakian BJ, Mavaddat N, Pickard JD, Robbins TW (2000) Methylphenidate enhances working memory by modulating discrete frontal and parietal lobe regions in the human brain. J Neurosci 20(6):RC65

Moeller S, Yacoub E, Olman CA, Auerbach E, Strupp J, Harel N, Uğurbil K (2010) Multiband multislice GE-EPI at 7 tesla, with 16-fold acceleration using partial parallel imaging with application to high spatial and temporal whole-brain fMRI. Magn Reson Med 63(5):1144–1153. https://doi.org/10.1002/mrm.22361

Mones E, Vicsek L, Vicsek T (2012) Hierarchy measure for complex networks. PLoS ONE 7(3):e33799. https://doi.org/10.1371/journal.pone.0033799

Morris A, Ravishankar M, Pivetta L, Chowdury A, Falco D, Damoiseaux JS, Diwadkar VA (2018) Response hand and motor set differentially modulate the connectivity of brain pathways during simple uni-manual motor behavior. Brain Topogr 31(6):985–1000. https://doi.org/10.1007/s10548-018-0664-5

Mueller S, Wang D, Fox MD, Yeo BT, Sepulcre J, Sabuncu MR, Liu H (2013) Individual variability in functional connectivity architecture of the human brain. Neuron 77(3):586–595. https://doi.org/10.1016/j.neuron.2012.12.028

Owen AM, McMillan KM, Laird AR, Bullmore E (2005) N-back working memory paradigm: a meta-analysis of normative functional neuroimaging studies. Hum Brain Mapp 25(1):46–59. https://doi.org/10.1002/hbm.20131

Papademetris X, Jackowski M, Joshi A, Scheinost D, Lacadie C, DiStasio M, Staib L (2017) BioImage Suite: An integrated medical image analysis suite, Section of Bioimaging Sciences, Dept. of Diagnostic Radiology, Yale School of Medicine (http://www.bioimagesuit.org)

Park HJ, Friston K (2013) Structural and functional brain networks: from connections to cognition. Science 342(6158):1238411. https://doi.org/10.1126/science.1238411

Passingham RE (2002) The frontal cortex: does size matter? Nat Neurosci 5(3):190–192. https://doi.org/10.1038/nn0302-190

Pavlopoulos GA, Secrier M, Moschopoulos CN, Soldatos TG, Kossida S, Aerts J, Bagos PG (2011) Using graph theory to analyze biological networks. BioData Min 4:10. https://doi.org/10.1186/1756-0381-4-10

Ravizza SM, Delgado MR, Chein JM, Becker JT, Fiez JA (2004) Functional dissociations within the inferior parietal cortex in verbal working memory. Neuroimage 22(2):562–573. https://doi.org/10.1016/j.neuroimage.2004.01.039

Robinson JL, Laird AR, Glahn DC, Lovallo WR, Fox PT (2010) Metaanalytic connectivity modeling: delineating the functional connectivity of the human amygdala. Hum Brain Mapp 31(2):173–184. https://doi.org/10.1002/hbm.20854

Rubinov M, Sporns O (2010) Complex network measures of brain connectivity: uses and interpretations. Neuroimage 52(3):1059–1069. https://doi.org/10.1016/j.neuroimage.2009.10.003

Ruxton GD, Beauchamp G (2008) Time for some a priori thinking about post hoc testing. Behav Ecol 19(3):690–693. https://doi.org/10.1093/beheco/arn020

Setsompop K, Gagoski BA, Polimeni JR, Witzel T, Wedeen VJ, Wald LL (2012) Blipped-controlled aliasing in parallel imaging for simultaneous multislice echo planar imaging with reduced g-factor penalty. Magn Reson Med 67(5):1210–1224. https://doi.org/10.1002/mrm.23097

Silverstein BH, Bressler SL, Diwadkar VA (2016) Inferring the dysconnection syndrome in schizophrenia: interpretational considerations on methods for the network analyses of fMRI data. Front Psychiatry 7:132. https://doi.org/10.3389/fpsyt.2016.00132

Sporns O (2011) The human connectome: a complex network. Ann NY Acad Sci 1224:109–125. https://doi.org/10.1111/j.1749-6632.2010.05888.x

Sporns O (2018) Graph theory methods: applications in brain networks. Dialogues Clin Neurosci 20(2):111–121

Stam CJ, Reijneveld JC (2007) Graph theoretical analysis of complex networks in the brain. Nonlinear Biomed Phys 1(1):3. https://doi.org/10.1186/1753-4631-1-3

Thirion B, Varoquaux G, Dohmatob E, Poline JB (2014) Which fMRI clustering gives good brain parcellations? Front Neurosci 8:167. https://doi.org/10.3389/fnins.2014.00167

Xu J, Moeller S, Strupp J, Auerbach E, Feinberg DA, Ugurbil K, Yacoub E (2012) Highly accelerated whole brain imaging using aligned-blipped-controlled-aliasing multiband EPI. Proc Int Soc Mag Reson Med 20:2306

Zuo XN, Ehmke R, Mennes M, Imperati D, Castellanos FX, Sporns O, Milham MP (2012) Network centrality in the human functional connectome. Cereb Cortex 22(8):1862–1875. https://doi.org/10.1093/cercor/bhr269